Mechanism of deactivation of Au/Fe$_2$O$_3$ catalysts under water–gas shift conditions

B. Aeijelts Averink Silberova, M. Makkee*, and J. A. Moulijn

DelftChemTech, Catalysis Engineering, Faculty of Applied Sciences, Delft University of Technology, Julianalaan 136, 2628 BL Delft, The Netherlands

The stability of Au supported catalysts for the water–gas shift reaction was studied. Two types of continuous flow experiments were performed, i.e. temperature-programmed and long-term isothermal stability test. The highest initial rate was obtained for catalysts used without any calcination or other high-temperature treatment. The continuous flow experiments showed that all Au/Fe$_2$O$_3$ catalysts deactivated under water–gas shift conditions. The deactivation trend occurred independently on the Au loading, the method of preparation, calcination or high-temperature treatment.

The various causes on the deactivation, i.e. the formation of carbon-containing species, the change of Au particles or changes of the support were investigated in terms of DRIFTS coupled with MS, TGA, TEM, N$_2$ physisorption, ICP, and XRD. Even though stable carbonate and carbonyl surface species were found on the spent catalysts, the quantity of these species indicated that they are not the main cause of the deactivation. Furthermore, the agglomeration of the Au particles was not severe and was not observed for all Au catalysts. The deactivation of Au/Fe$_2$O$_3$ was mainly caused by the change of the support. A significant reduction of the surface area of the support is taking place during the water–gas shift reaction as a function of time on stream. This decrease of the surface area can almost solely explain the decrease on the catalytic activity.

KEY WORDS: water-gas shift; gold; Au/Fe$_2$O$_3$; stability; deactivation.

1. Introduction

The water–gas shift (WGS) reaction is a key reaction in the production for hydrogen for a number of processes in refineries as well as in chemical synthesis. Moreover, the WGS reaction plays a key role in novel applications such as the partial removal of CO in hydrogen feedstock for fuel cell (PEM) applications [1]. The reactions are industrially carried out using two types of catalysts: Fe–Cr and Cu–Zn operating between 350–500 and 180–250 °C, respectively [2]. These catalysts are pyrophoric and are not suitable for use in residential or automotive fuel processors. A great interest is, therefore, nowadays in finding alternative catalysts that are not pyrophoric and exhibit a good performance, including a high stability [3,4].

Recently, it has been reported that Au supported catalysts are interesting candidates for novel WGS applications [4–12]. High activity of Au/CeO$_2$ has been observed by Andreeva *et al.* [5] and Fu *et al.* [6]. Increasing the Au loading causes higher CO conversion although no large difference has been observed at high temperatures [5]. High CO conversion, above 95%, has been also reported for Au/Fe$_2$O$_3$ and Au/ZrO$_2$ by Tabakova *et al.* [7]. The catalytic activity decreases when gold is deposited on amorphous [7] or not well-crystallized supports [6,7]. Furthermore, the catalytic performance for the WGS has been improved by

addition of Ru to Au supported on hydroxyapatite [8,9] or by addition of ZrO$_2$ to Au/Fe$_2$O$_3$ [10].

Catalyst deactivation, the loss of catalytic activity and/or selectivity over time, is of crucial importance in the industrial application. There are several causes for deactivation and they generally can be classified into main three categories: chemical (e.g. poisoning), thermal (e.g. thermal degradation, sintering), and mechanical (e.g. fouling, carbon deposition) [13–15].

It has been shown that most of the Au supported catalysts deactivate under WGS conditions [6,7,10,12,16]. This will affect the commercial aspects of gold catalysis [17]. One of the main reasons of deactivation mentioned in the recent studies is the formation of carbonyl or carbonate-like species leading to blockage of the active surface sites [6,12]. In Au–CeO$_2$ catalytic systems, stability problems have been assigned to the formation of cerium oxide-hydroxycarbonate [6]. It is reported that the activation of the Au catalysts contaminated by carbonates can be fully restored after heating the deactivated catalysts in air at elevated temperatures [12].

Some of the studies have considered sintering of Au particles as a reason for the deactivation [6,9,10,16]. Change of Au particle size from 4 to 5.5 nm has been taken as a significant change influencing the catalytic performance [16].

In studies of Tabakova *et al.* a substantial reduction of the pore volume has been postulated as a reason for the lower catalytic activity and fast deactivation of the

* To whom correspondence should be addressed.
E-mail: m.makkee@tudelft.nl

Au supported catalyst in the WGS reaction [7]. Similarly, Fu *et al.* have reported that the initial loss of activity observed under reaction conditions could be correlated to the loss of ceria surface [6].

In the present work, temperature-programmed and long-term stability tests of Au/Fe_2O_3 catalysts for the water–gas shift reactions were performed. The various causes of deactivation were investigated in detail by applying the different characterization techniques (e.g. DRIFTS, MS, TGA, TEM, BET, XRD) to as-received and spent catalysts at different times on stream. Formation of carbonate and carbonyl species, sintering, loss of Au and change of Fe_2O_3 support will be discussed.

2. Experimental

2.1. Catalyst preparation

Au/Fe_2O_3 catalysts were supplied by Cardiff University, Salford University, and World Gold Council (WGC) via the European network Auricat. Fe_2O_3 was prepared and supplied by Cardiff University. The preparation method used for similar samples supplied by Cardiff University is described in detail elsewhere [18,19]. Details about the estimation of gold loadings and BET area of these samples were reported previously [20]. The preparation method used for similar samples supplied by Salford University was described elsewhere [21]. The catalyst supplied by World Gold Council is referred as a reference Au catalyst [22]. The Cu-based commercial catalyst was supplied by (former ICI) Johnson Matthey. All the samples were pressed, crushed, and sieved to give a particle size of 212–355 μm. The loading of Au was determined by ICP. In case of the reference WGC catalyst, the samples had already been calcined at 400 °C. All samples were used either as received, i.e. non-calcined, or were high-temperature treated (HTT) at 300 °C or 400 °C in a He flow for 30 min. The heating rate for HTT was set to 10 °C/min. The preparation method, Au loading, HTT temperature and BET of all catalyst are given in Table 1.

2.2. Catalytic testing

The steady-state WGS experiments were performed in the six-flow reactor setup. The setup allows testing of six samples simultaneously under the same reaction conditions. A detailed description of this setup was described elsewhere [23]. The samples (50 mg) were placed in the middle of the quartz reactors (i.d. 4.0 mm) and held by a sintered glass and two quartz wool plugs. The reactor furnace was controlled with a Eurotherm 2604. The pressure in each reactor was set to 1 bar. The gases, He (100%) and CO (100%) were used without further purification and were fed from independent Bronkhorst F-201C mass flow controllers. Distilled H_2O

was fed via the liquid mass flow controller and was introduced to the CO/He flow before entering the individual reactors. Gas compositions of the reaction mixture were typically 0.5% CO, 1.5% H_2O vapour and 98% He. A typical flow of reaction mixture in each reactor was 55 mL/min. The effluent mixtures, typically consisting of CO, H_2O, CO_2, and H_2, were analysed with a gas chromatograph (Chrompack CP 9001) equipped with a thermal conductivity detector, with the use of a Poraplot Q column and a Molsieve 5 A column. Two types of the catalytic testing protocols were followed, *viz.* temperature-programmed and longer-term isothermal conditions.

2.2.1. Temperature-programmed test

During the temperature-programmed test, the reactors were heated (10 °C/min) in He flow to 100 °C. At this temperature, the reaction mixture was introduced and after a certain stabilization time, effluents of each reactor were analysed in succession. Once the analyses at 100 °C were finished, the furnace temperature was automatically raised (10 °C/min) by 30 °C. Analysis was performed at each 30 °C temperatures interval up to 250 °C. Subsequently, the analogous protocol was followed, reducing the temperature from 250 to 100 °C. Subsequently, the reactors were cooled down under He flow. The temperature profile is shown in figure 1.

2.2.2. Isothermal stability test at 200 °C

First, the reactors were heated (10 °C/min) in He flow to 200 °C. The reaction mixture was introduced at this temperature and each reactor was frequently analysed in succession in duration of 40 h. At the end, the reactors were cooled down under He flow. A schematic presentation of the temperature profile followed in this experiment is shown in figure 1.

2.3. Diffuse reflectance infrared Fourier spectroscopy (DRIFTS) and mass spectrometry

Diffuse-reflectance infrared Fourier transform spectroscopy (DRIFTS) experiments were performed on a Thermo Nicolet Nexus IR with OMNIC software. Infrared spectra were recorded with co-addition of 64 scans and applying a resolution of 4 cm^{-1}. A Pfeiffer Vacuum ThermoStar mass spectrometer allowed a direct identification of mass fragments of the reactants and products after interaction with the catalyst sample in the DRIFT cell.

2.3.1. Identification of (adsorbed) species present

Infrared spectra were recorded against KBr spectra for the identification of adsorbed species present on the surface. The spectra were recorded under an inert flow of He (35 mL/min) at 25 °C.

Table 1
The catalyst used for steady-state water–gas shift reaction performed in six-flow set-up

	Supplied by	Preparation method[a]	Au loading (%)	HTT[b] at temperature (°C)	BET (m²/g)
Au/Fe₂O₃–C-as received	Cardiff University	Co-p	3.4[c]	–	203
Au/Fe₂O₃–C-300HTT (300c)	Cardiff University	Co-p	3.4[c]	300	143 ± 5
Au/Fe₂O₃–C-400HTT	Cardiff University	Co-p	3.4[c]	400	45
Fe₂O₃–C-as received	Cardiff University	–	–	–	172
Fe₂O₃–C-400HTT	Cardiff University	–	–	–	51
Au/Fe₂O₃–S-as received	Salford University	Dp	1	–	48 ± 2
Au/Fe₂O₃–S-300HTT	Salford University	Dp	1	300	47 ± 2
Au/Fe₂O₃–W-as received[d]	World Gold Council	Co-p	4.48[c]	–	38.7
Au/Fe₂O₃–W-400HTT[d]	World Gold Council	Co-p	4.48[c]	400	38.7

[a] Co-p = co-precipitation, Dp = deposition-precipitation performed at pH = 7.5
[b] HTT = High-temperature treatment performed at 300 °C or 400 °C for 30 min in flow of He, heating rate: 10°C/min
[c] Estimated by ICP
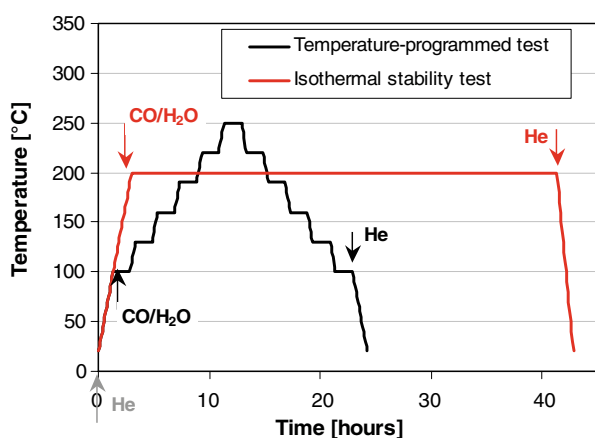[d] Calcination at 400 °C performed by supplier

Figure 1. Temperature profiles applied for steady-state water–gas shift experiments in the six-flow set-up.

2.3.2. Operando spectroscopy

When the sample was exposed to a reaction gas or mixture, infrared spectra were recorded against the background of the sample under flowing He at 25 °C. The total flow rate of 32.2 mL/min was applied when the catalyst (~50 mg) was further exposed to a reaction gas or mixture. CO/Ar (20% CO in Ar) was diluted by He to obtain a 0.5% CO. The mixing device connected to the IR cell was equipped with a four-way valve, allowing switching between a by-pass line for an inert gas and a main line for the reaction mixture.

2.4. Thermo gravimetric analysis (TGA)

Thermo gravimetric analyses were performed on TGA/SDTA851e equipped with the sample robot TSO801RO and the gas controller Mettler Toledo TSO800GC1. After a stabilization period of 30 min, samples were heated (10 °C/min) to 900 °C under flowing He or air. A Pfeiffer Vacuum ThermoStar mass spectrometer allowed a direct identification of the mass fragments of the desorbing species. TG analyses of the as-received samples and the samples that had been used in stability tests were performed.

2.5. Transmission electron microscopy (TEM)

Transmission electron microscopy identified the size and distribution of the Au particles. Powder samples were crushed between two glass slides and positioned onto a lacey carbon coated copper 'finder' grid with the aid of a micromanipulator. The samples were examined in the Tecnai F20 transmission electron microscope using the following instrumental conditions: voltage (kV) = 200, C2 aperture (m) = 30–50, Modes: Bright Field (BF), high-angle annular dark field (HAADF) imaging, energy dispersive X-ray analyses. TEM analyses of the as-received and spent samples were performed by Johnson Matthey.

2.6. Volumetric N₂ physisorption

Prior to the N₂ physisorption and desorption measurements, the samples were dried in vacuum at 100 °C in order to remove present moisture and other volatile components. The as-received samples, which had not been high-temperature treated, were dried at 200 °C. After pre-treatment adsorption and desorption isotherms were measured at 77 K on the Quantachrome Autosorb-6B. Information on the BET surface area, the pore size distribution and micro-pore contribution were deduced.

2.7. XRD

X-ray diffraction (XRD) was applied to identify crystalline phases inside as-received and spent catalysts. The samples were measured with Cu Kα radiation.

3. Results

3.1. Catalytic performance

3.1.1. Temperature-programmed test

The conversion of CO obtained via the water–gas shift reaction over various Au/Fe_2O_3 catalysts and Fe_2O_3 is presented as a function of the temperature in figure 2a and b. The highest CO conversion was observed for the as-received Au/Fe_2O_3 catalyst, which had not been treated at high-temperature. The mild high-temperature treatment (300 °C) caused slightly lower conversion of CO. For more severe HTT (400 °C) the conversion of CO was reduced by a factor of two. The consequence of the high-temperature treatment on the catalytic performance was noticed for all the Au catalysts, independently of details of procedures or Au loading.

The beneficial effect of Au on the water–gas shift activity of Fe_2O_3 was clearly shown by the blank experiment when only Fe_2O_3 was applied (figure 2a). The maximum CO conversion (~4%) obtained at 250 °C was one to two orders of magnitude lower compared to the Au supported catalysts.

Figure 2b shows furthermore the results of the Cu-based catalyst, commonly applied commercially. At high temperatures (> 200 °C), the CO conversion was higher than those of the investigated Au supported catalyst, whereas at the lower temperature Au-based catalysts are more active.

The comparison of the Au supported catalysts reveals that different shapes of curves were obtained for Au/Fe_2O_3 (figure 2a and b). The sample of Au/Fe_2O_3 received from Salford University has a different temperature-dependence curve than the Au/Fe_2O_3 supplied by Cardiff University and the World Gold Council.

Figure 3 gives preliminary information on the stability. For nearly all Au-based catalysts lower CO conversions were obtained in the cooling-down programme, except the one supplied by the World Gold Council. In case of the Cu-based catalyst, the stability is relatively high.

3.1.2. Isothermal stability test at 200 °C

The long-term experiments performed at 200 °C are shown in figure 4. The results show deactivation for all gold-supported catalysts, independently on the Au loading, the choice of the preparation method and additional pre-treatments. The deactivation rate of no high-temperature treated Au catalysts was higher than the ones that had been high-temperature treated at 300 °C or 400 °C.

The lowest activity but the best stability was obtained with a reference catalyst supplied by the World Gold Council. The highest activity with an excellent stability
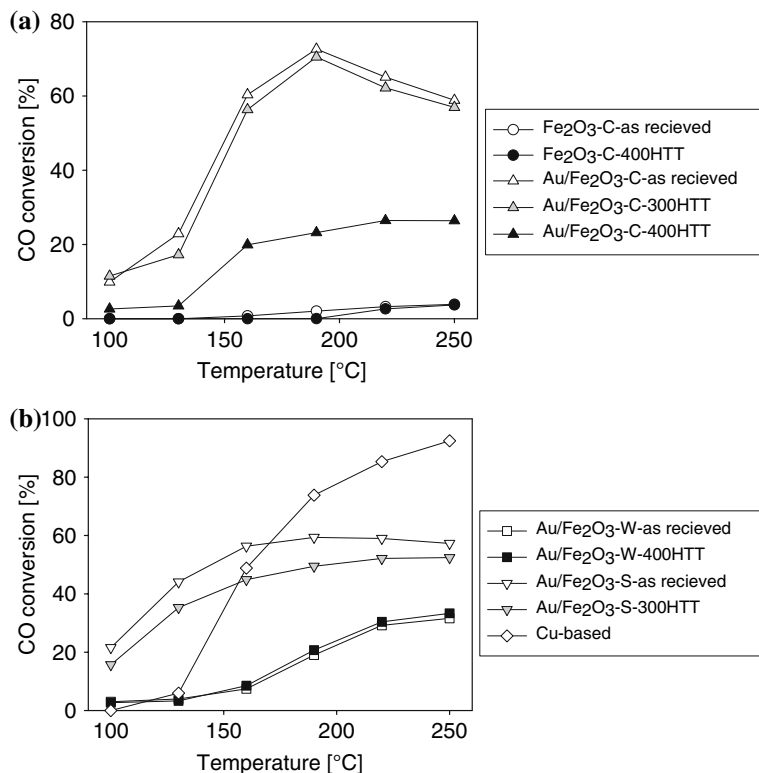

Figure 2. CO conversion obtained during the temperature-programmed test of the water–gas shift reaction over Au/Fe_2O_3, Fe_2O_3 and Cu-based catalysts. The experiments were run in six-flow set-up. Cardiff catalysts (**a**). World Gold Council catalysts, Salford catalysts and commercial Cu based reference catalyst (**b**).
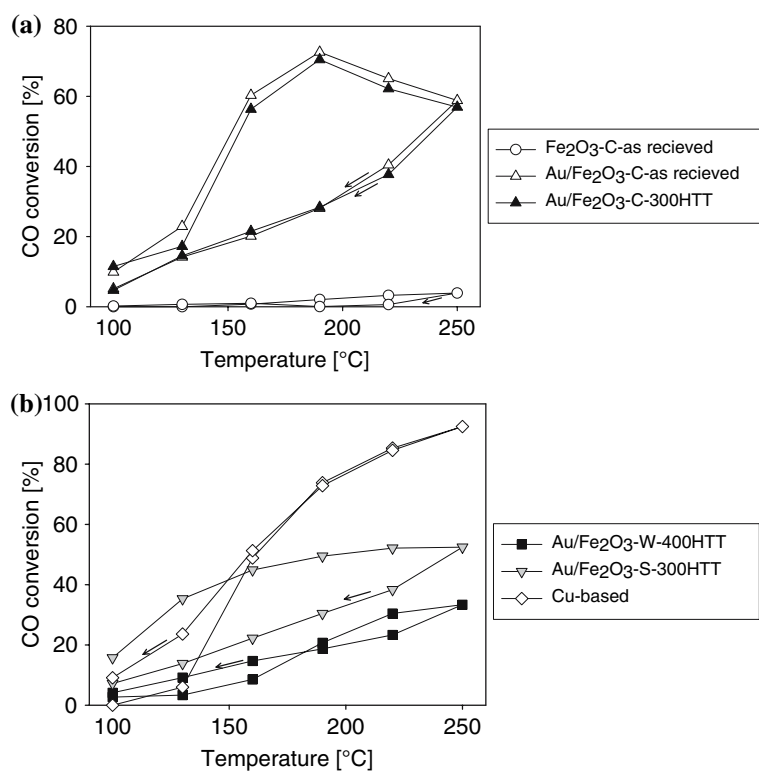
Figure 3. Comparison of the CO conversion obtained during the increasing and decreasing branch of the temperature-programmed protocol of the water–gas shift reaction over Au/Fe₂O₃, Fe₂O₃ and Cu-based catalysts. The experiments were run in six-flow set-up.

for the water–gas shift was achieved with the Cu-based catalyst, a commercially available low-temperature WGS catalyst. It has to be stated that the activation procedure for this commercial catalyst was not applied. It has followed the activation procedure for the gold catalysts.

3.2. DRIFTS and MS

3.2.1. Identification of (adsorbed) species

The DRIFT spectrum of the as-received Au catalyst (Cardiff) is shown in figure 5a. The bands indicating the occurrence of the carbonate-like species in the 1700–900 cm^{-1} range, are clearly present. It is also clear that the samples contain hydroxyl groups (1640 cm^{-1}, 3700–3100 cm^{-1}) [24]. The spectrum of the Au catalyst (calcined at 400 °C) supplied by the World Gold Council reveals that carbonate-like species are present in relatively small quantities (figure 5b).

For the spent catalysts the major difference is the nearly absence of bands indicating water molecules or hydroxyl groups. The Cardiff catalyst shows bands of high intensities in the carbonate region (1700–900 cm^{-1}) and absorbance of metal carbonyl complexes (carbon monoxide complexes) in the lower part of the region 2300–1900 cm^{-1} [24]. The spent World Gold Council catalyst contains similar adsorbed species (figure 5b).

3.2.2. Exposure to CO at 25 °C

The amount of oxygen available for the conversion of CO to CO₂ was investigated when the catalyst was exposed to CO at room temperature. The evolution of CO₂ during the exposure of Au/Fe₂O₃–C-as received to CO is shown in figure 6a.

The spent Cardiff catalyst showed qualitatively the same behaviour, but the amount of CO₂ evolved was much less (figure 6b). The DRIFT spectrum (figure 5a) nicely shows that this spent catalyst contained only a limited amount of hydroxyl groups and the data in figure 6b that the same applies to the accessible surface oxygen needed for the conversion of CO. The same experiments were performed for the as-received and spent World Gold Council catalysts. Also in this case a limited amount of CO₂ was recorded when the spent catalyst was exposed to CO and a significant lower amount of hydroxyl groups was recorded by DRIFTS (figure 5b).

Elsewhere it is shown that CO was gradually converted into CO₂ via the formation of carbonate and bicarbonates, which decompose during the reaction [25]. These steps occur at the Au-support interface in the presence of the hydroxyl groups and the available surface oxygen [25]. The bulk diffusion of oxygen in Fe₂O₃ structure potentially results in refilling the upper layer with bulk oxygen [25].
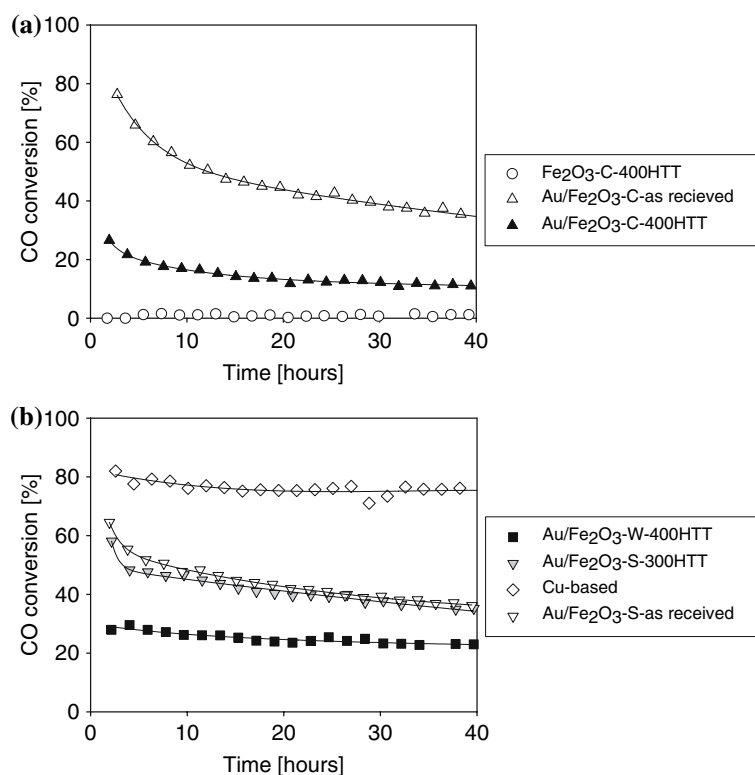
Figure 4. CO conversion obtained during the isothermal stability test of the water–gas shift reaction over Au/Fe_2O_3, Fe_2O_3 and Cu-based catalysts. The experiments were performed at 200 °C in the six-flow set-up.

3.3. TGA

Thermo gravimetric analyses of Au/Fe_2O_3–W-as received and -spent in the temperature-programmed tests were performed in He flow (He-TGA) to indicate desorption of present adsorbed species and in air (air-TGA) to give information about an effect of oxygen on decomposition of the present species.

Desorption of CO_2 recorded during He-TGA is shown in figure 7a. A peak of CO_2 was recorded below 100 °C. A small amount of desorbing of CO_2 was detected around 250 °C. The mass spectroscopy signal of H_2O shown in figure 7b indicates that the as-received samples contain adsorbed molecular water and/or hydroxyl groups. The desorption of H_2O showed a maximum at 95 °C and at higher temperature gradually decreases with rising temperature to 900 °C.

In case of the spent catalyst, CO_2 started to desorb only above 200 °C with a maximum release at 330 °C and additional partial increase with a maximum at 560 °C. The water signal did not differ much from the one for the as received catalyst.

The loss of carbon-containing species and water or hydroxyl group molecule corresponds to the weight loss of as-received and spent catalyst (figure 7c). For both catalysts, the initial decrease of the weight is assigned to desorption of water. A minimum is observed at 330 °C for the spent catalyst. This agrees with the maximum on the CO_2 signal. The calculated weight loss is 1.84% and

0.87% for the as-received and spent catalyst, respectively.

TG analysis of the as-received catalyst performed in air shows a similar CO_2 desorption signal as for TGA-He (figure 8a). The amount of CO_2 recorded during air-TGA of the spent catalyst was higher compared to the as-received catalyst and was released at a higher temperature (> 180 °C). CO_2 desorption from the as-received catalyst and the spent catalyst was accompanied by a release of H_2O (figure 8b).

Air-TGA analysis indicates that the weight loss of the as-received sample was 2.0% (figure 8c). In case of the spent catalyst, the total catalyst weight increases during the air-TGA by approximately 0.44%. The increase of the weight is clearly shown in figure 9c and in agreement with the observation during the mass spectrometry analysis where the O_2 signal was followed. The signal of oxygen decreases with a minimum at exactly the same temperature. A direct linkage between the weight increase and the observed change of the oxygen signal is apparent.

3.4. TEM

Au particle sizes on the as-received and spent catalysts in the water–gas shift were estimated in terms of TEM. Figure 9 gives the micrographs for the as received and the spent World Gold Council catalysts. Figure 9a and b shows that the diameter of the Au particles of the
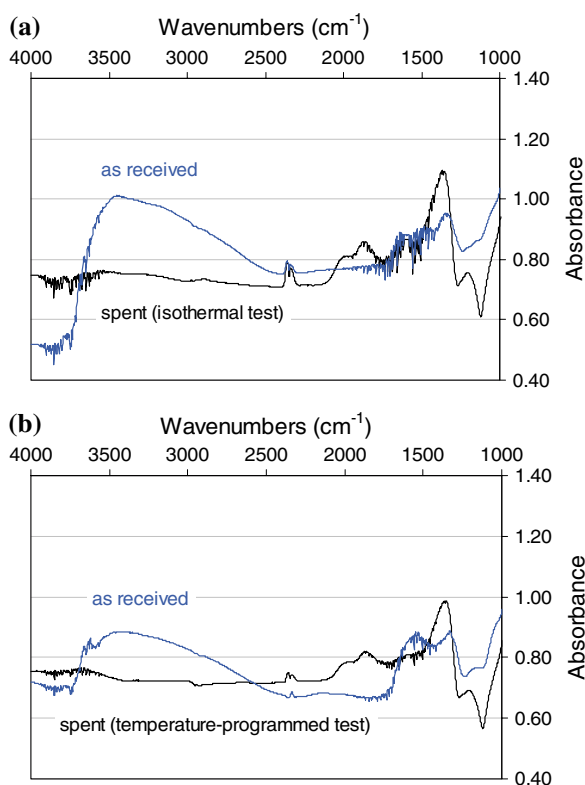
Figure 5. The spectra are recorded against KBr spectra DRIFT spectra of Au/Fe$_2$O$_3$–C-as received and -spent in the isothermal stability test at 200 °C (**a**) and of Au/Fe$_2$O$_3$–W-as received and -spent in the temperature-programmed test (**b**).

Figure 6. Evolution of CO and CO$_2$ during the exposure of Au/Fe$_2$O$_3$–C-as received (**a**) and Au/Fe$_2$O$_3$–C-spent in the isothermal stability test (**b**) to CO at 25 °C.

as-received catalyst is between 2 and 5 nm. The Au particles are very well dispersed. Once the catalyst was exposed to the temperature-programmed test, the size of Au particles did not change significantly, except for some occasional Au particles of 15–30 nm diameters (figure 9c and d). Similar size and distribution of Au particles were noticed for the spent catalysts in the isothermal stability test at 200 °C (figure 9e and f).

The data for the other catalysts are summarized in Table 2. The simple conclusion can be drawn that the size distribution does not change, both during HTT (up to 400 °C) and the two reaction protocols.

3.5. ICP

The results of ICP analyses of the as-received and -spent catalysts are presented in Table 3. During reaction the Au content is not changed.

3.6. Textural properties

The results of N$_2$ adsorption measurements (Table 4) indicate that the as-received and the spent samples are mesoporous materials. The Cardiff catalyst shows the highest BET area. For the other catalysts BET is much lower. The BET area did not decrease significantly once the catalyst was calcined at 300 °C but severely for the
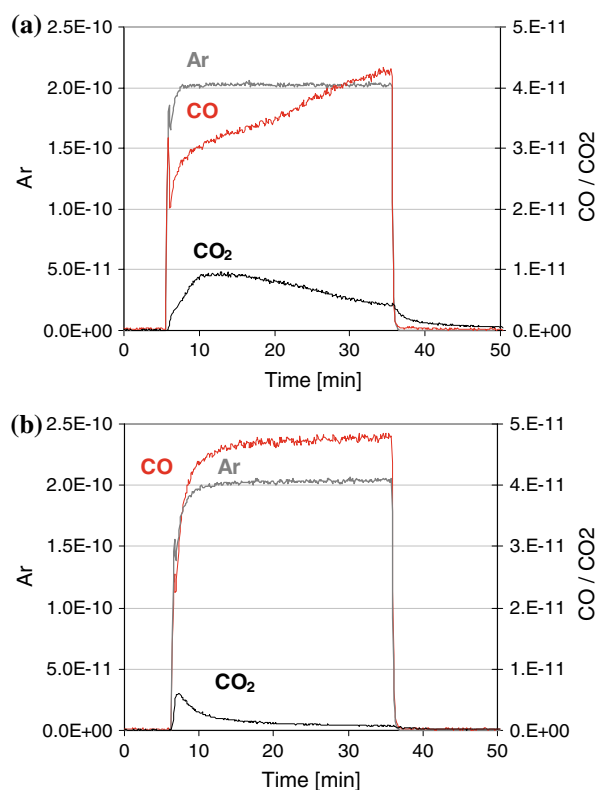
catalyst calcined at 400 °C. During the reaction the BET surface area decreases and the pore size increases. The re-oxidation of the spent catalysts led to no further decrease in the BET surface area.

3.7. XRD

According the XRD results (figure 10a–c), the fresh 300 °C-calcined Cardiff and WGC catalysts are in form of hematite (α-Fe$_2$O$_3$), while magnetite (Fe$_3$O$_4$) is found for the fresh 300 °C-calcined Salford catalyst. Other sharp peaks could be identified as calcite (CaCO$_3$) like or another carbonate containing species on the fresh Cardiff catalyst. The support of all spent catalysts consists of the reduced form, i.e. magnetite. Re-oxidation of the spent catalyst the magnetite structure was transformed into the hematite structure.

4. Discussion

4.1. Catalytic performance

Among the as received non-calcined Au-based catalysts the order in activity was Au/Fe$_2$O$_3$–C > Au/Fe$_2$O$_3$–S. This difference can be explained at least partly from the different Au loading (figure 2).
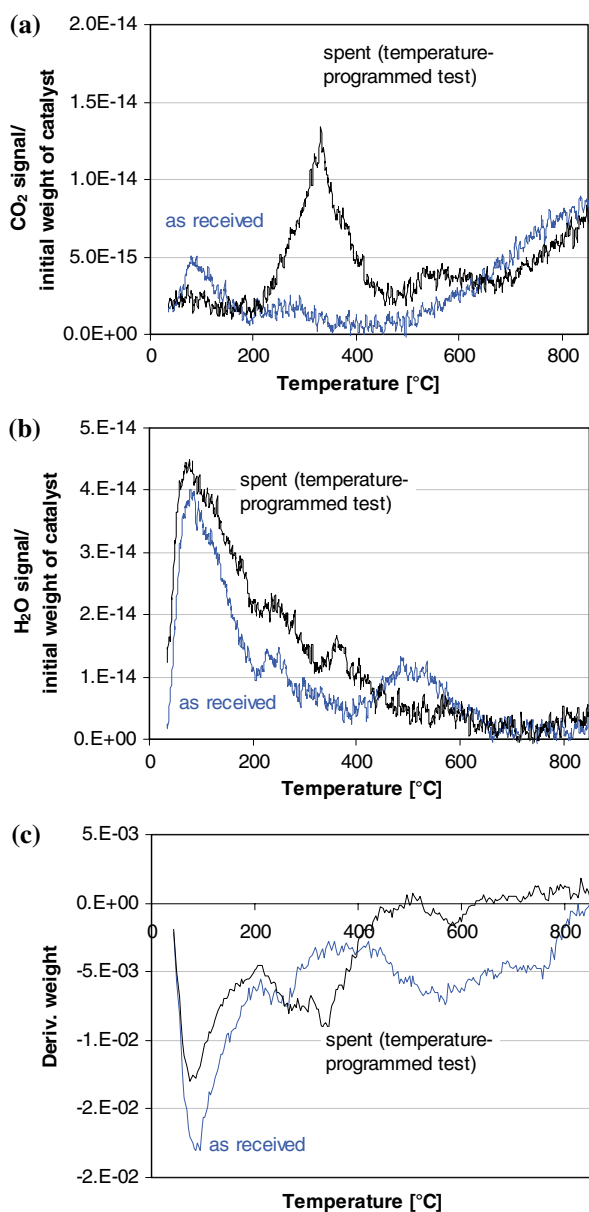
Figure 7. He-TGA of Au/Fe$_2$O$_3$–C-as received and -spent in the temperature-programmed test. CO$_2$ (**a**) and H$_2$O (**b**) signals are related to the initial weight of the catalysts (**c**). Heating rate: 10 °C/min.

Figure 8. Air-TGA of Au/Fe$_2$O$_3$–C-as received and -spent in the temperature-programmed test. CO$_2$ (**a**) and H$_2$O (**b**) signals are related to the initial weight of the catalysts (**c**). Heating rate: 10 °C/min.

Once these catalysts were high-temperature treated, especially above 300 °C, the catalytic performance was severely lowered (figure 2b). The results with the World Gold Council catalyst are consistent with this observation. This catalyst had been calcined by the supplier and the observed activity is low. A similar conclusion has been published earlier [20,21].

The temperature-programmed and isothermal stability tests revealed that Au supported catalysts are unstable under the water–gas shift conditions (figure 3a and b). An exception was the World Gold Council catalyst. The explanation is that the high calcinations temperature already had caused extensive deactivation.
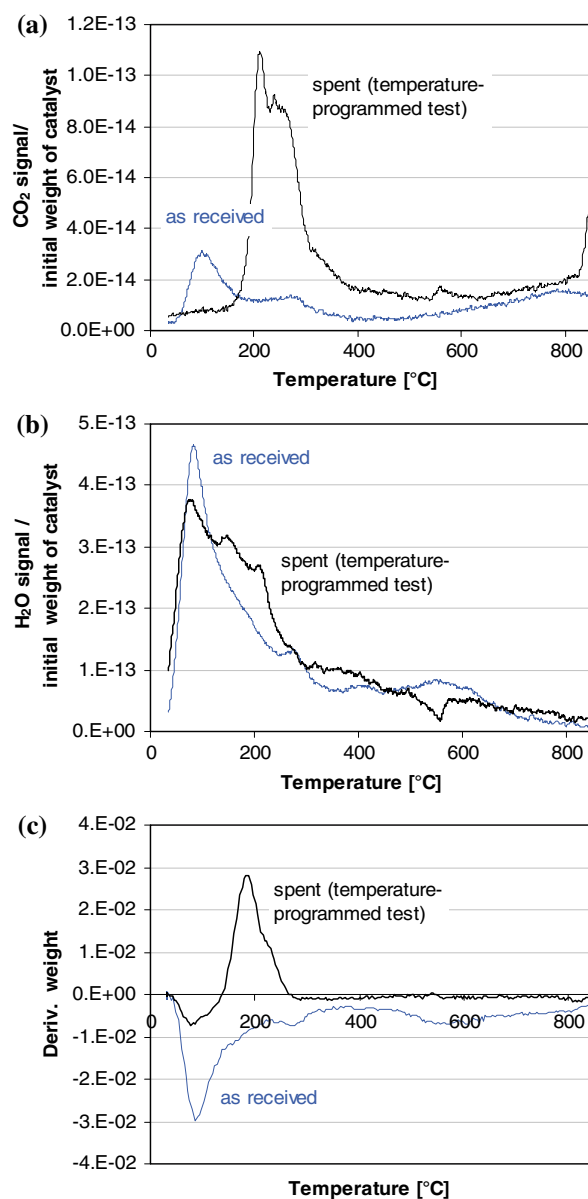
The comparison with the commercial Cu catalyst reveals that this is the superior system: it exhibits the highest activity and stability, although the initial activity of the Au-based catalysts is promising. The problem, obviously, is the low stability of the Au-based catalysts. In order to analyse the underlying mechanism the spent catalysts were investigated in terms of the formation of carbon-containing species and hydroxyl groups, changes of the Au particles, i.e. agglomeration, and changes of the support Fe$_2$O$_3$.
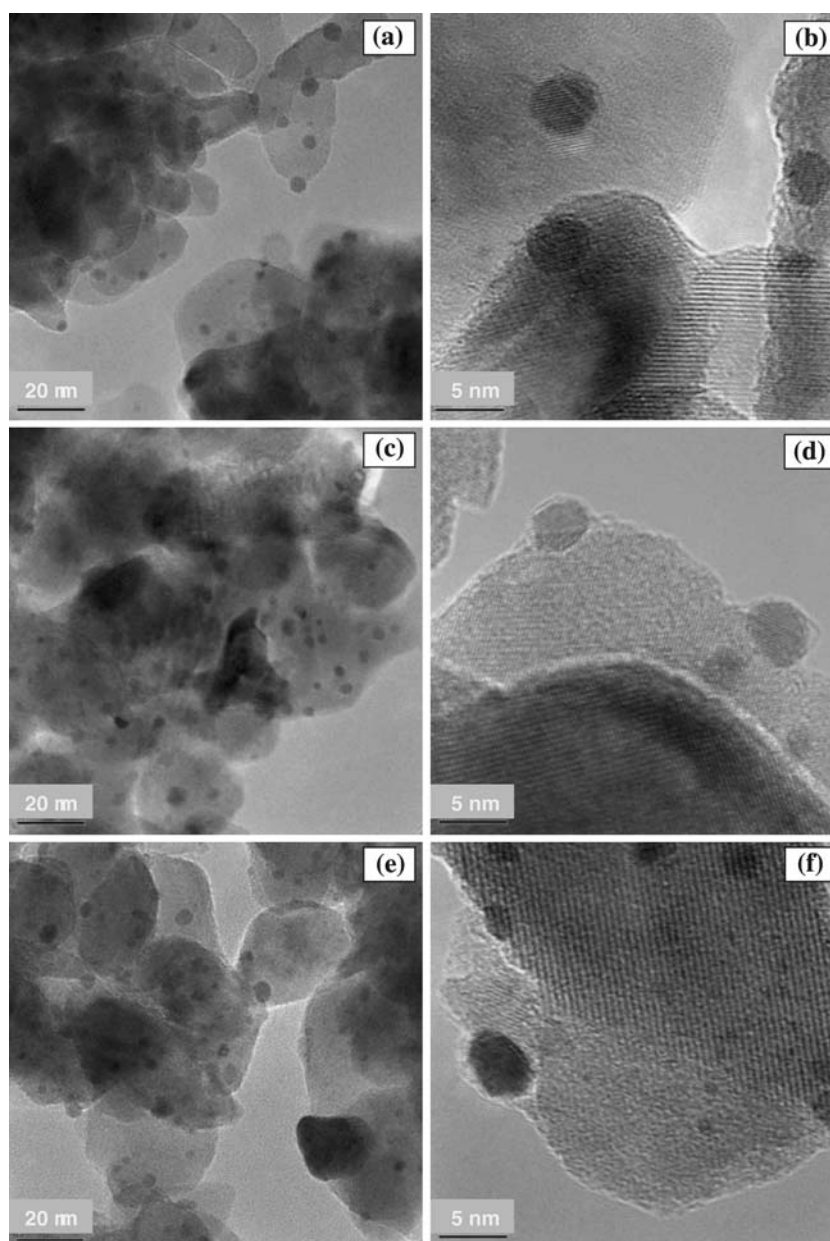
Figure 9. TEM images of Au/Fe$_2$O$_3$–W-as received (**a**, **b**), Au/Fe$_2$O$_3$–W-spent in the temperature-programmed test (**c**, **d**), Au/Fe$_2$O$_3$–W-spent in the isothermal stability test (**e**, **f**).

Table 2
The size and size distribution of Au particles of as-received and spent Au/Fe$_2$O$_3$ catalysts estimated by TEM

	Au particle size and distribution
Au/Fe$_2$O$_3$–W-as received	2–5 nm, well dispersed
Au/Fe$_2$O$_3$–W-spent temperature-programmed test	2–5 nm, well dispersed and occasionally 15–30 nm
Au/Fe$_2$O$_3$–W-spent isothermal stability test	2–5 nm, well dispersed and occasionally 15–30 nm
Au/Fe$_2$O$_3$–C-as received	10–80 nm
Au/Fe$_2$O$_3$–C-spent temperature-programmed test	Frequently 5–10 nm and 20–50 nm
Au/Fe$_2$O$_3$–C-400HTT-spent isothermal stability test	Frequently 5–10 nm and 20–50 nm
Au/Fe$_2$O$_3$–S-as received	Occasionally 10–50 nm
Au/Fe$_2$O$_3$–S-300HTT-spent temperature-programmed test	Frequently 5–20 nm
Au/Fe$_2$O$_3$–S-300HTT-spent isothermal stability test	Frequently 5–10 nm

Table 3
The Au loading of as-received and spent Au/Fe$_2$O$_3$ catalysts estimated by ICP

	Au loading (wt%)
Au/Fe$_2$O$_3$–W-as received	4.26 ± 0.21
Au/Fe$_2$O$_3$–W-spent temperature-programmed test	4.46 ± 0.22
Au/Fe$_2$O$_3$–W-spent isothermal stability test	4.48 ± 0.22
Au/Fe$_2$O$_3$–C-as received	3.10 ± 0.16
Au/Fe$_2$O$_3$–C-spent temperature-programmed test	3.46 ± 0.17
Au/Fe$_2$O$_3$–C-spent isothermal stability test	2.97 ± 0.15
Au/Fe$_2$O$_3$–S-as received	0.72 ± 0.04
Au/Fe$_2$O$_3$–S-spent temperature-programmed test	0.69 ± 0.03
Au/Fe$_2$O$_3$–S-spent isothermal stability test	0.70 ± 0.04

4.2. Carbonate-like species and hydroxyl groups

4.2.1. Initially present carbonate-like species

DRIFT spectra of the as-received catalysts reveal that all gold samples contained carbonate species (figure 5a and b). The intensity of the bands at wave numbers 1700–900 cm^{-1}, however, decreased for the spent catalysts. This supports the observation in our previous studies showing that initially present carbonate species remaining after the high-temperature treatment are removed once the catalyst is exposed to CO [25].

Moreover, the cleaning up of the catalyst surface from the initially present carbonate species was also observed by TGA. The results indicate that the carbonate species were removed already during heating the sample in flowing He. It is interesting that the decomposition of these species was promoted in the presence of air (figure 8a). Furthermore, the TGA study showed that the spent catalysts had lost carbonate-type species under the conditions of the WGS reaction.

It was also noted that one of the present carbonates could be in form of the calcite (CaCO$_3$) as observed by XRD (figure 10). Once exposed to the water–gas shift reaction, the XRD results indicated that no CaCO$_3$ crystals are present.

4.2.2. Formation of carbonate-like species during reaction

Bands ($\sim$1390 cm^{-1}) assigned to the carbonate-like species were visible in DRIFT spectra of the spent catalyst (figure 5a and b). In the as-received samples these bands were less intense. An increase of the bands in wave numbers 2300–1900 cm^{-1} characteristic for the presence of strongly bounded carbonyl groups (figure 5a and b) [24] was also noticed for the spent catalysts compared to the fresh ones. The TGA data showed that the decomposition of carbonate-like species resulting in CO$_2$ release took place above 200 °C during the heating in He and above 180 °C in air. The broader temperature range, additional CO$_2$ release and higher signal of CO$_2$ during TGA in air indicate that some types of the formed carbonate-like species are decomposed only in the presence of oxygen.

It is shown that the newly formed carbonate and carbonyl species are observed only during the water–gas shift reaction. These were formed independently on the Au loading, the methodology of the catalyst preparation or the type of the experiment (temperature-programmed or isothermal stability). A question is, however, whether the build-up of carbonate-like species is a main cause of the decreasing activity during the continuous flow experiments. Several research ascribed the formation of (hydroxy)carbonates and/or formates as a severe cause of the deactivation of Au/CeO$_2$ during the WGS [6,12]. Significant amounts of deposited material, up to 10–20% of the catalyst weight are frequently obtained [13]. From the TGA experiments we estimate that the amounts deposited are less than 1%. Furthermore, by comparing the deactivation behaviour of the Au/Fe$_2$O$_3$–C spent catalyst (decrease from 78% to less than 40%) with that of the Au/Fe$_2$O$_3$–W-400c spent catalyst (hardly any deactivation) no obvious difference in the

Table 4
The results of the N$_2$ physisorption of as-received and spent Au/Fe$_2$O$_3$ catalysts

	BET (m^2/g)	Total pore volume (cm^3/g)	Pore diameter[a] (nm)
Au/Fe$_2$O$_3$–W-as received	38.7	0.14	10
Au/Fe$_2$O$_3$–W-300HTT-spent temperature-programmed test	27 ± 1	0.20	25
Au/Fe$_2$O$_3$–W-300HTT- spent isothermal stability test	31[a]	0.25[a]	35[a]
Au/Fe$_2$O$_3$–C-as received	203	–	–
Au/Fe$_2$O$_3$–C-spent temperature-programmed test	34 ± 1	0.18	19
Au/Fe$_2$O$_3$–C-spent isothermal stability test	31[a]	0.28[a]	20[a]
Au/Fe$_2$O$_3$–C-300c	143 ± 5	0.27	5 + 8
Au/Fe$_2$O$_3$–C-300HTT-spent temperature-programmed test	39 ± 2	0.18	15
Au/Fe$_2$O$_3$–S-as received	47 ± 2	0.13	11
Au/Fe$_2$O$_3$–S-spent isothermal stability test	31 ± 1	0.15	18

The values were estimated by N$_2$ adsorption except when indicated otherwise
[a] Estimated by Kr adsorption. The deviation compared to the values measured by N$_2$ is less than 10% relative
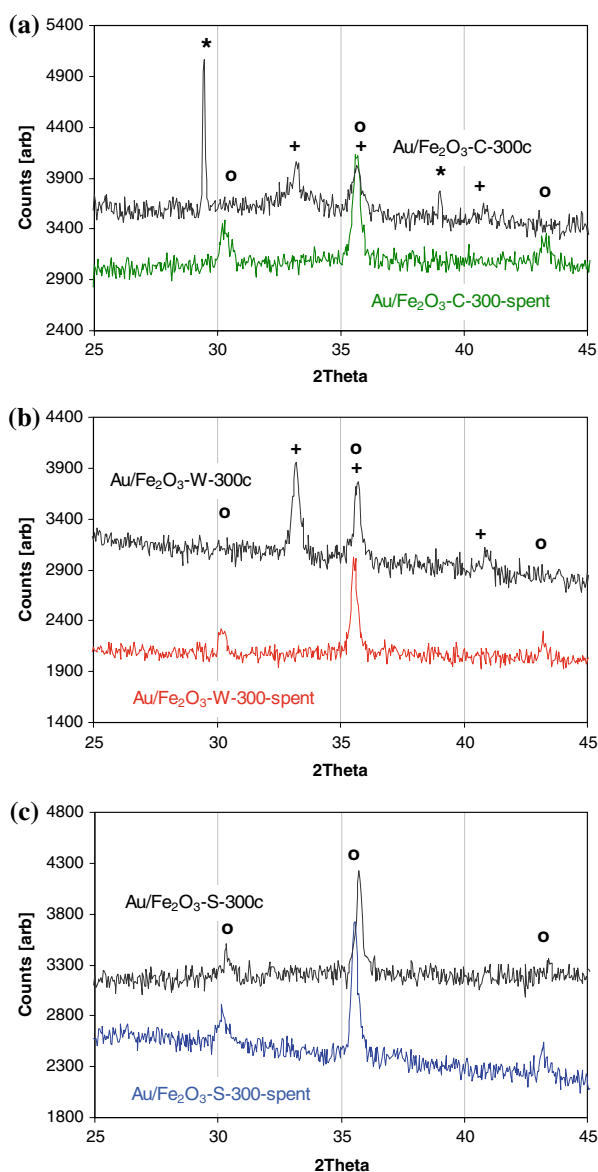
Figure 10. XRD analyses of the Au/Fe$_2$O$_3$–C-300c and Au/Fe$_2$O$_3$–C-300-spent (a), the Au/Fe$_2$O$_3$–W-300c and Au/Fe$_2$O$_3$–W-300-spent (b) and the Au/Fe$_2$O$_3$–S-300c and Au/Fe$_2$O$_3$–S-300-spent (c). The spent catalysts had been subjected to the temperature-programmed test. + 1 hematite; o magnetite; ★ calcite

Figure 11. The rate of CO$_2$ production versus BET surface area. Full square: Au/Fe$_2$O$_3$–C-as received, half full square: Au/Fe$_2$O$_3$–C-300HTT, empty square: Au/Fe$_2$O$_3$–C-as received, full triangle: Au/Fe$_2$O$_3$–WGC-as received, empty triangle: Au/Fe$_2$O$_3$–WGC-400 HTT. Full: stability test (first and last points), empty and half full: temperature-programmed test (higher value = maximum value, lower value = value at 190 °C).

indeed, the high amount of carbonates are removed, nevertheless, the loss of the catalyst has been negative, i.e. the weight of the catalyst increases (figure 8c). MS analysis showed that the weight increase is accompanied by a decrease of the O$_2$ signal. So, we conclude that the spent Au/Fe$_2$O$_3$ can be in minor extent regenerated by the removal of the carbonates but in this case more significantly by the re-oxidation of the Fe support in the oxygen atmosphere.

4.2.3. Hydroxyl groups

The as-received Au/Fe$_2$O$_3$ catalysts contain a high amount of adsorbed water and hydroxyl groups (figure 5a and b) that were removed during the water–gas shift reaction, as apparent from the DRIFTS spectra (figure 5a and b) and the TGA experiments (figures 7b and 8b). Desorption of H$_2$O was observed during both He-TGA as well as air-TGA even though the presence oxygen promote the release of H$_2$O.

It is remarkable that although the catalyst was exposed to H$_2$O during the water–gas shift reaction, the amount of hydroxyl groups was remarkably lower on the spent catalyst than on the as-received catalyst (figure 5a and b).

4.3. Changes of Au particles during reaction

Except for the World Cold Council catalyst, the size of the Au particles after exposure to the water–gas shift conditions remained in the range observed for the Au particle size on the as-received catalyst or no particle size changes were observed (Table 2). The results of TEM of all the selected Au/Fe$_2$O$_3$ catalysts indicate that larger Au particles are not formed on every Au/Fe$_2$O$_3$ catalysts tested, whereas deactivation was observed for every Au/Fe$_2$O$_3$ catalyst. So, agglomeration of Au particles can occur to a certain extent; nevertheless it will not be a main cause of the deactivation of Au/Fe$_2$O$_3$ during the WGS.

intensities of the carbonate bands in the DRIFTS spectra is observed. In addition, the comparison of the weight loss observed during TGA of the as-received sample was higher (1.84%) than one with the spent catalyst (0.87%). These observations lead to a statement that newly formed stable carbonyl and carbonate-species during the water–gas shift cannot be the main cause of the Au/Fe$_2$O$_3$ deactivation.

Kim and Thompson assigned the deactivation of Au/CeO$_2$ to the formation of carbonates and formates not only due the observed species by the FT-IR and XPS techniques but also by the full regeneration of the catalyst after treatment in dry air at 400 °C for 4 h [12]. According our air-TGA of the spent Au/Fe$_2$O$_3$ catalyst,
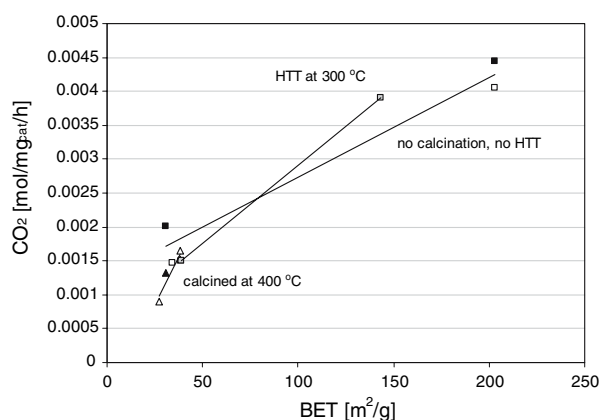
ICP analysis (Table 3) showed that no loss of Au during the WGS took place.

4.4. Changes of the support during the WGS

The support of the Au/Fe_2O_3–C-as-received and Au/Fe_2O_3–W-as-received was present in the oxidized form, i.e. Fe_2O_3 (figure 10a and b). The results obtained by XRD analyses showed that Fe_2O_3 was reduced to magnetite (Fe_3O_4) during reaction. Consistent with this observation, the support in Au/Fe_2O_3–S-as received consisting of the magnetite remains to be magnetite under reaction conditions. It is concluded that the catalytic activity of the Au supported on hematite or magnetite were not very different, but the state of the support during the water–gas shift is magnetite.

A decrease of the surface oxygen on the support during the reaction was observed from MS analysis of the CO_2 response on adding a CO step function by comparing as received and spent catalysts. Lower CO_2 production on the spent catalyst can be also due to the lower amount of hydroxyl groups being important for CO conversion to CO_2 at room temperature [25].

The re-oxidation of the spent catalysts was noticed during the TGA (air, 200 °C) of the spent catalyst. According to the results of N_2 physisorption, reduction of the surface area is an important process: it takes place upon calcination and under reaction conditions. Even the Au/Fe_2O_3, which had been calcined at 400 °C and had rather low surface area, the surface area decreased significantly during the reaction. The loss of the surface area also corresponded to an increase of the total pore volume and the pore diameter (Table 4).

The above discussion suggests a rather simple interpretation for the deactivation mechanism. The mechanism is not the formation of deposits formed e.g., by carbonate formation or changes in dimensions of the Au particles. The deactivation is accompanied by a change in textural properties. The simplest interpretation would then be a correlation between activity and surface area. This hypothesis was checked as follows.

From the step response MS experiments a CO_2 production rate can be calculated involving CO oxidation by surface oxygen. These rates related to the amount of the catalyst were calculated for fresh and spent Au catalysts in the isothermal stability or temperature-programmed test. The data are shown as a function of the BET area in figure 11. It is obvious that the rate nicely correlates with the surface area: it increases with increasing BET surface area. The correlation is not strictly linear according to a straight line through the origin. This is not surprising. In the two quite different deactivation protocols the catalyst undergoes massive changes and it is well conceivable that details of the deactivation conditions have influence on the local chemistry at the surface.

The support of the Au/Fe_2O_3 used for the water–gas shift reaction was severely transformed. In case that support is present in the form of hematite, the support is reduced to magnetite. Although water is present in the reaction mixture, the re-oxidation of the support does not occur to a large extent and the support remains in its reduced formed. This observation supports our proposed WGS mechanism at high temperatures presented in our previous study [25]. The production of carbon dioxide and hydrogen takes via the reduction-oxidation cycles where the re-oxidation of the support (Fe_2O_3) is the rate-limiting step [25].

5. Conclusions

The highest CO conversion was obtained with the non-calcined Au/Fe_2O_3. The calcination or high-temperature treatment lowered the surface area and consequently the catalytic activity. Deactivation was observed for all Au supported catalyst, independently on the Au loading, the method of preparation, the pre-treatment method or the crystalline structure of the supports.

The deactivation of Au/Fe_2O_3 appears to comprise several processes. The formation of carbonate and carbonyl species occurs to some extent and some agglomeration of Au particles takes place on the Au/Fe_2O_3 during the water–gas shift, but they are not seen as the main cause of the Au/Fe_2O_3 deactivation.

The support suffers of severe changes during the water–gas shift reaction. In case that the fresh Au catalyst is supported on hematite, the support is reduced to the magnetite. The water–gas shift reaction over Au/Fe_2O_3 occurring via reduction-oxidation mechanism where the re-oxidation of the support appears to be a rate-limiting step. The significant loss of the surface area of the support is taking place during the water–gas shift reaction affects the catalytic performance and will be the main cause of the Au/Fe_2O_3 deactivation.

In comparison with the commercial copper based WGS catalysts there is still a major issue for the gold based WGS catalysts in terms of stability.

Acknowledgments

References

[1] D.L. Trimm, Appl. Catal. A 296 (2005) 1.
[2] C. Rhodes, G.J. Hutchings and A.M. Ward, Catal. Today 23 (1995) 43.

[3] W. Ruettinger, O. Ilinich and R.J. Farrauto, J. Power Sources 118 (2003) 61.

[4] A. Kuperman and M.E. Moir, US Patent: US2005276741 (2005).

[5] D. Andreeva, V. Idakiev, T. Tabakova, L. Ilieva, P. Falaras, A. Bourlinos and A Travlos, Catal. Today 72 (2002) 51.

[6] Q. Fu, W. Deng, H. Saltsburg and M. Flytzani-Stephanopoulos, Appl. Catal. B 56 (2005) 57.

[7] T. Tabakova, V. Idakiev, D. Andreeva and I. Mitov, Appl. Catal. A 202 (2000) 91.

[8] A. Venugopal and M.S. Scurrell, Appl. Catal. A 245 (2003) 137.

[9] A. Venugopal, J. Aluha, D. Mogano and M.S. Scurrell, Appl. Catal. A 245 (2003) 49.

[10] J. Hua, Q. Zheng, Y. Zheng, K. Wei and X. Lin, Catal. Lett. 102 (2005) 99.

[11] G.C. Bond, Catal. Today 72 (2002) 5.

[12] C.H. Kim and L.T. Thompson, J. Catal. 230 (2005) 66.

[13] R. Hughes, *Deactivation of Catalysts* (Academic Press, 1984).

[14] C.H. Bartholomew, Appl. Catal. A 212 (2001) 17.

[15] J.A. Moulijn, A.E. Diepen and F. Kapteijn, Appl. Catal. A 212 (2001) 3.

[16] L. Luengnaruemitchai and Osuwan, Catal. Commun. 4 (2003) 215.

[17] C.W. Corti, R.J. Holliday and D.T. Thompson, Appl. Catal. A 291 (2005) 253.

[18] N.A. Hodge, C.J. Kiely, R. Whyman, M.R.H. Siddiqui, G.J. Hutchings, Q.A. Pankhurst, F.E. Wagner, R.R. Rajaram and S.E. Golunski, Catal. Today 72 (2002) 133.

[19] R.M. Finch, N.A. Hodge, G.J. Hutchings, A. Meagher, Q.A. Pankhurst, F.E. Siddiqui, M.R.H. Wagner and R. Whyman, Phys. Chem. Chem. Phys. 1 (1999) 485.

[20] S.T. Daniells, A.R. Overweg, M. Makkee and J.A. Moulijn, J. Catal. 230 (2005) 52.

[21] F. Moreau, G.C. Bond and A.O. Taylor, J. Catal. 231 (2005) 105.

[22] D. Cameron, R. Holliday and D. Thompson, J. Power Sources 118 (2003) 298.

[23] J. Pérez-Ramírez, R.J. Berger, G. Mul, F. Kapteijn and J.A. Moulijn, Catal. Today 60 (2000) 93.

[24] N.B. Colthup, L.H. Daly, S.E. Wiberley, *Introduction to Infrared and Raman Spectroscopy*, third ed. (Academic Press, 1990).

[25] B. Aeijelts Averink Silberova, G. Mul, M. Makkee and J.A. Moulijn, J. Catal. 243 (2006) 171.